Defects Associated with Nanostructures in AlZnMg and AlCu(Mg) Alloys

R. Ferragut
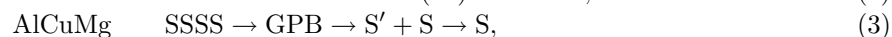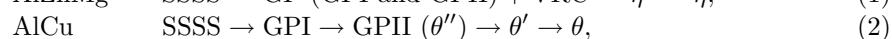
INFM, Dipartimento di Fisica. L-NESS — Politecnico di Milano
Via Anzani 52, 22100 Como, Italy

The present work reports on a positron annihilation study addressing the structural and chemical characterization of solute aggregates containing open volumes (vacancies and/or misfit regions at precipitate–matrix interfaces) in AlZnMg, AlCu, and AlCuMg alloys. High resolution transmission electron microscopy results for selected ageing conditions are also presented. Two main points are discussed: (i) differentiation of the origin of hardening during artificial ageing between the AlZnMg and AlCu(Mg) alloy systems; (ii) structural origin of secondary ageing at low temperature, after a few minutes of high temperature exposure. It is shown that in AlZnMg alloys hardening at a high temperature is concomitant with the loss of coherency; on the contrary, in AlCu(Mg) alloys hardening is associated with coherent structures. Positron lifetime and coincidence Doppler broadening data taken during secondary ageing indicate that the residual solute supersaturation leads to the formation of coherent Zn–Mg–v (or Cu–Mg–v) aggregates.

PACS numbers: 78.70.Bj, 81.40.Cd

1. Introduction

A century has elapsed since Alfred Wilm made the discovery of age hardening in an aluminium alloy that became known as duralumin [1]. Presently, wrought alloys most extensively used in the aircraft industry are based on AlZnMg and AlCuMg. These materials display a very good response to age hardening [2]. The precipitation sequence of these systems can be condensed in the following formulas (see details in Ref. [2]):

$$\text{AlZnMg} \qquad \text{SSSS} \rightarrow \text{GP (GPI and GPII)} + \text{VRC} \rightarrow \eta' \rightarrow \eta, \qquad (1)$$
$$\text{AlCu} \qquad \text{SSSS} \rightarrow \text{GPI} \rightarrow \text{GPII} \ (\theta'') \rightarrow \theta' \rightarrow \theta, \qquad (2)$$
$$\text{AlCuMg} \qquad \text{SSSS} \rightarrow \text{GPB} \rightarrow \text{S}' + \text{S} \rightarrow \text{S}, \qquad (3)$$

where the supersaturated solid solution SSSS is obtained after solution treatment and quenching. Depending on the composition and the dimension of the solute atoms different kinds of coherent Guinier−Preston zones (GP) could be formed.

VRC are vacancy rich clusters of Zn. The intermediate precipitates are the semi-coherent phases η', θ' (θ''), and S', and η, θ, and S are the stable phases of each alloy.

It is well known that the response to artificial ageing of the AlZnMg system is significantly enhanced by pre-ageing, carried out at temperatures below the solvus of GP zones. On the contrary, pre-ageing at a low temperature after quenching does not improve the mechanical properties of the AlCu(Mg). This is not the only difference between the AlZnMg and AlCu(Mg) alloy systems: the products of precipitation that contribute to the maximum hardening are different. In the present work positron spectroscopy contributes to elucidate these differences by giving information on the coherence degree of the nanostructures formed. These results are corroborated by high resolution transmission electron microscopy (HRTEM).

For many years there was an implicit acceptance that, once an alloy had been hardened by ageing at an elevated temperature, its mechanical properties would remain stable at a significantly lower temperature. Recently, it has been demonstrated by positron annihilation spectroscopy (PAS) that solute–vacancy complexes may remain mobile at room temperature (RT) when aged aluminium alloys are cooled from a higher temperature (secondary ageing) [3, 4]. It has also been shown that thermal treatments that include a stage of secondary ageing improve significantly (up to 20%) the peak hardness and other mechanical properties of aluminium alloys [5]. The results presented in this work are consistent with the formation of new coherent precipitates during secondary ageing in the studied alloys.

2. Experimental

The results reported below concern four alloys, AlZnMg-C, AlCuMg-C, AlCuMg, and AlCu, whose chemical compositions are shown in Table in atomic percent. The letter C at the end of the abbreviation of two ternary alloys means commercial alloys. AlZnMg-C is the 7012 alloy (very similar to the 7075 alloy) and AlCuMg-C is the 2024 alloy.

TABLE

Chemical composition of the studied alloys in at.%.

	Zn	Cu	Mg	Mn	Fe	Si	others
AlZnMg-C	2.6	0.4	2.3	0.05	< 0.13	< 0.15	< 0.07
AlCuMg-C	< 0.1	1.8	1.6	0.2	< 0.09	< 0.05	< 0.07
AlCuMg	–	2.0	0.6	–	–	–	–
AlCu	–	1.7	–	–	–	–	–

The specimens were solution treated in an air circulating furnace, the respective conditions being: 2 h at 470°C for AlZnMg-C, 5 h at 482°C for AlCuMg-C,

20 min at 500°C for the AlCuMg alloy, and 30 min at 520°C for the AlCu alloy. At the end of the solution treatment, the samples were water quenched at RT (in ice-water in the case of AlCu and AlCuMg-*C*). The AlZnMg-*C* samples were pre-aged at RT for 5 days after solution treatment and quenching, all other samples were brought to the high temperature immediately after quenching. Artificial ageing was performed in a glycerine oil bath at 150°C (also at 190°C for AlCuMg). Secondary ageing was studied in AlZnMg-*C*, AlCuMg and AlCu alloys by means of positron lifetime spectroscopy at temperatures up to 70°C after few minutes of artificial ageing.

PAS measurements were performed with a 20 μCi source of ^{22}NaCl deposited on a thin kapton foil (7.5 μm) which was sandwiched between two identical alloy specimens. Positron lifetime spectroscopy (LS) and coincidence Doppler broadening (CDB) spectroscopy were adopted. Both techniques are sensitive to the chemical environment of open volume defects in age-hardening alloys. CDB enables to detect the first neighbour atoms of open volume defects, specially Zn or Cu atoms in the studied alloys. The lifetime spectrometer was a fast-fast timing coincidence system with a time resolution (FWHM) of 255 ps. After subtracting the source component, the spectra with about 10^6 coincidences were satisfactorily analysed as a single lifetime component. In some cases, the separation of two components was also possible, but this required the use of constraints derived from the application of the trapping model with specific hypotheses on the annihilation process. To avoid the risk of over-interpreting the data, only results from free one-component fits are reported below, with the caveat that the apparent single lifetime has the meaning of an average over unresolved complex lifetime spectra. CDB measurements were performed via two intrinsic Ge detectors in timing coincidence. Coincidence events at energies E_1 and E_2 were collected in a 512×512 matrix, with about 4×10^7 counts accumulated in 60 hours. The coincidence events located on a thin strip (≈ 1.3 keV wide) centred on the $E_1 + E_2$ matrix diagonal were used for obtaining the one-dimensional distribution ρ of the longitudinal component of the momentum of the electron–positron (e–p) pair $p_L = (E_1 - E_2)/c$. The resulting peak-to-background ratio was 10^5:1 and the momentum resolution (FWHM of the spectrum measured along the $E_1 - E_2$ matrix diagonal) was $\approx 3.7 \times 10^{-3} m_0 c$.

The HRTEM observations were carried out in a Philips CM200UT transmission electron microscope, operating at 200 kV. The images were obtained along the [001] and [011] zone axes. Specimens with 3 mm in diameter and 0.2 mm thickness were thinned by double-jet electropolishing with a 30% HNO_3 solution in methanol at -25°C and 10 V.

3. Results and discussion

3.1. Age-hardening

Figure 1 shows the evolution of the positron lifetime as a function of the ageing time at 150°C in alloys AlZnMg-*C*, AlCuMg-*C*, and AlCu. The evolution of
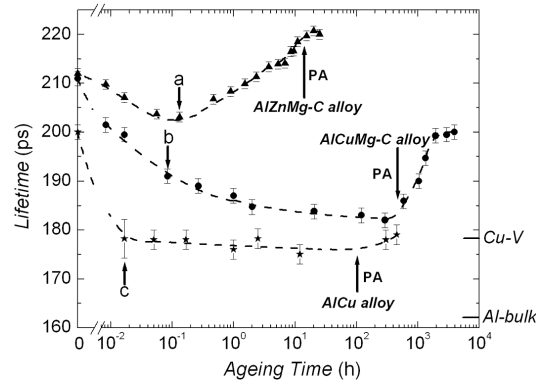
Fig. 1. Evolution of the positron lifetime in AlZnMg-*C* (▲), AlCuMg-*C* (∘) and AlCu (⋆) during artificial ageing at 150°C. The label PA indicates for each alloy the ageing time corresponding to maximum hardness (peak-ageing condition). Letters *a*, *b*, and *c* indicate the thermal conditions of the samples studied by CDB. Positron lifetimes in bulk Al and in vacancies in pure Cu are indicated on the right vertical axes.

the positron lifetime can be schematically divided in three stages for the AlZnMg-*C* alloy and in four stages for the two AlCu(Mg) alloys.

- AlZnMg-*C*: (i) initial drop up in the first minutes of ageing (correlated, not simultaneous, with hardening decrease [3]); (ii) progressive increase (correlated with the hardening of the alloy up to the peak-ageing condition [3]) and (iii) weak reduction in correspondence with over-ageing (stage of decreasing hardness).

- AlCuMg-*C* and AlCu: (i) initial drop in the first minutes of ageing (concomitant with an increasing hardness, which is very important in AlCuMg-*C* [6, 7]); (ii) progressive decrease (corresponding to the hardness plateau in AlCuMg-*C* [6], and to the hardening increase in AlCu); (iii) further slower decrease extended over the peak-hardening region and (iv) increase at the beginning of the over-ageing stage.

The stage of the initial positron lifetime drop was further investigated by means of CDB. The CDB distributions of Fig. 2, presented here as relative variations with respect to bulk Al, show the differences between the initial condition of ageing (0 min) and stages *a* and *b* in Fig. 1, which correspond to 8 min and 5 min of ageing at 150°C respectively, in AlZnMg-*C* (parts (a) and (a′)) and in AlCuMg-*C* (parts (b) and (b′)). By comparing the curves in Fig. 2 it may be observed that the CDB distributions of AlZnMg-*C* and AlCuMg-*C* for 0 min at 150°C are markedly different at high momentum (> 1 a.u.), where the contribution of positron annihilation with Zn or Cu 3*d* electrons is important. This difference confirms the formation after or during quenching of VRC that contains Zn atoms in the AlZnMg alloy system [8]. There is almost no influence of pre-

-ageing (5 days at RT) on the CDB distributions at high momentum in the case of AlZnMg-C (open triangles in part (a) of Fig. 2). After a few minutes of ageing at 150°C the CDB high momentum distribution is increased, the effect being most important for the AlCuMg-C alloy. A similar (but less strong) effect was observed for the AlCu alloy (see Ref. [9]). At low momentum (lower parts (a′) and (b′)), where the contribution of positron annihilation with Mg electrons is expected, CDB distributions decrease in both alloys after high temperature ageing.
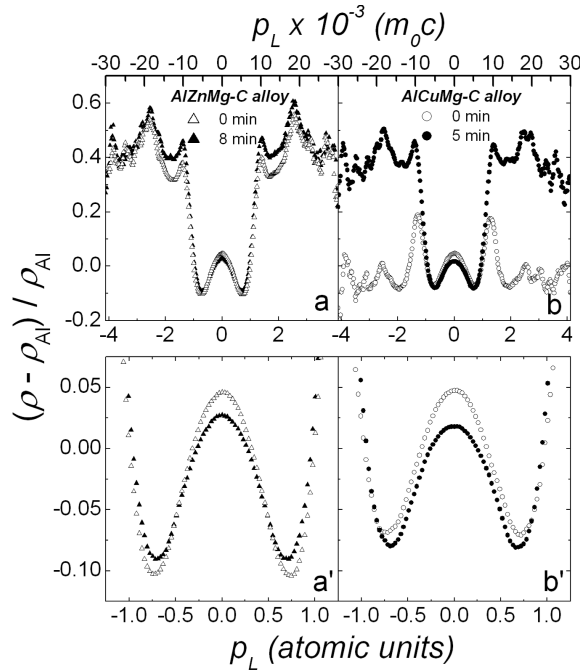

Fig. 2. CDB distributions (relative difference to bulk Al) for AlZnMg-C and AlCuMg-C. Parts (a) and (a′): AlZnMg-C alloy after solution treatment, quenching, pre-ageing 5 d at RT ($\triangle$) plus an additional ageing at 150°C for 8 min ($\blacktriangle$), corresponding to label a in Fig. 1. Part (b) and (b′): AlCuMg-C alloy after solution treatment and quenching ($\circ$), plus additional ageing at 150°C for 5 min ($\bullet$), corresponding to label b in Fig. 1. The lower parts (a′) and (b′) show a zoom of the low momentum part of the CDB distributions.

On combining LS and CDB results, it may be concluded that the drop of the positron lifetime in the first minutes of ageing in Fig. 1 is correlated with a change in the average chemical composition surrounding the positron traps. The results of Fig. 2 indicate that, after holding the alloy a few minutes at a high temperature, the nanostructures seen by positrons contain more Cu (or Zn) atoms and less Mg atoms near to the vacancies.

Figure 3 shows HRTEM images taken for samples near to peak ageing conditions, and show the particles that mainly contribute to the hardening in the AlZnMg [2] and AlCuMg [10] systems. Figure 3a refers to AlZnMg-C; the contrast is due to semicoherent η' precipitates [11]. Figure 3b is for AlCuMg-C; in this micrography, the dominant structure at peak ageing can be attributed to coherent solute aggregates.
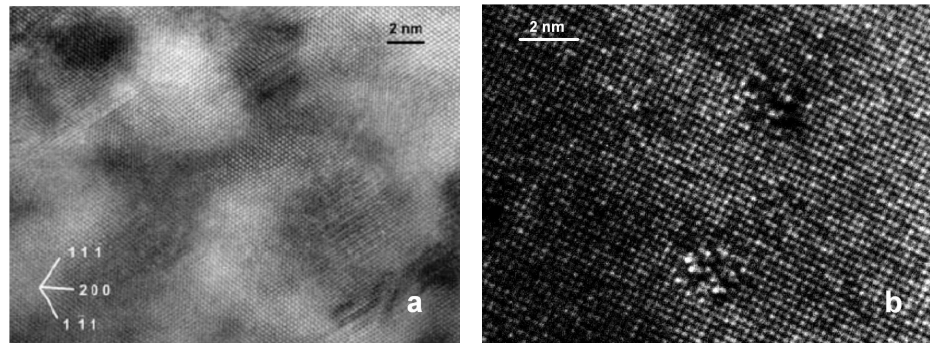

Fig. 3. HRTEM images of artificial aged samples near the peak-ageing conditions. Part (a): image of the AlZnMg-C alloy obtained along the $\langle 011 \rangle$ zone axes (after Ref. [11]). Part (b): image of the AlCuMg-C alloy obtained along the $\langle 001 \rangle$ zone axes.

Hardening in AlCu and AlCuMg-C alloys begins before the onset of the positron lifetime increase that is associated to the formation of misfit interfaces. In fact, the lifetime data of Fig. 1 indicate that the loss of coherency occurs at times near to those corresponding to peak hardness (i.e., at the beginning of overageing). This idea is supported by the HRTEM results of Fig. 3, consistently with the view that hardening at 150°C is associated with coherent aggregates [10]. On the contrary, the comparison of the positron lifetime data with the hardness--time curve indicates that in AlZnMg-C the loss of coherency occurs before the onset of hardening.

3.2. Secondary ageing

Figure 4 shows the results of lifetime measurements obtained during secondary ageing after 1, 5, and 8 min of artificial ageing in AlCu, AlCuMg, and AlZnMg-C, respectively. The solid lines through the experimental points shown in Fig. 4 are the result of a fitting based on a trapping-model calculation discussed in Ref. [4]. This model implies that the initial stage of a rapid variation of positron lifetime is determined by the reduction of the fraction of positrons trapped at vacancies decorated by Cu (or Zn) atoms, while the slower part comes from a progressive atomic reorder. It is worth mentioning that the lifetime evolution observed in the AlCu alloy is entirely different from the non-monotonic curves of the ternary AlCuMg and AlZnMg-C alloys. This comparison is consistent with ascribing the
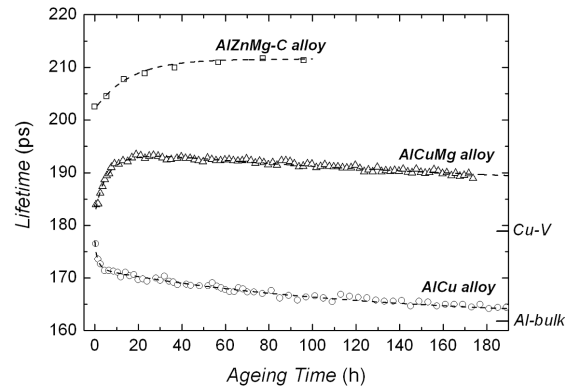
Fig. 4. Evolution of the positron lifetime of the AlZnMg-*C*, AlCuMg, and AlCu alloys during secondary ageing. The conditions of the measurements were: for AlZnMg-*C*, secondary ageing at 70°C starting from the condition labelled *a* in Fig. 1 (8 min at 150°C); for AlCuMg, secondary ageing at RT after 5 min of ageing at 190°C; for AlCu alloy secondary ageing at 60°C starting from the condition labelled *c* in Fig. 1 (1 min at 150°C). Positron lifetimes in bulk Al and in vacancies in pure Cu are indicated on the right vertical axes.

non-monotonic trend to a fast aggregation of Mg to preexisting vacancy–Cu (or vacancy–Zn) clusters, followed by a further aggregation of Cu (or Zn) that takes place with a slower kinetics [4, 12].

It is clear, from all the evidence reported here and in previous works [12, 13], that secondary ageing at low temperature implies the re-formation of coherent nanoparticles (GP zones or coherent solute clusters). The process is effective only if sufficient supersaturation is left after the interruption of the preliminary heating at high temperature.

Acknowledgments

References

[1] A. Wilm, *German Patent* DRP244554 (1906).

[2] I.J. Polmear, *Light Alloys*, 3rd ed., Arnold, London 1995.

[3] R. Ferragut, A. Somoza, A. Dupasquier, *J. Phys. Condens. Matter* **8**, 8945 (1996).

[4] A. Somoza, A. Dupasquier, I.J. Polmear, P. Folegati, R. Ferragut, *Phys. Rev. B* **61**, 14454 (2000).

[5] R.N. Lumley, I.J. Polmear, A.J. Morton, *International Patent Application* PCT/AU00/01601 (2000) and PCT/AU02/00234 (2002).

[6] R. Ferragut, A. Somoza, A. Dupasquier, I.J. Polmear, *Mater. Sci. Forum* **396-402**, 777 (2002).

[7] R.N. Lumley, I.J. Polmear, A.J. Morton, *Mater. Sci. Forum* **396-402**, 893 (2002).

[8] H. Löffler, Y. Kovacs, J. Lendvai, *J. Mater. Sci.* **18**, 2215 (1983).

[9] R. Ferragut, A. Dupasquier, G. Ferro, M. Biasini, A. Somoza, *Mater. Sci. Forum* **445-446**, 75 (2004).

[10] S.P. Ringer, T. Sakurai, I.J. Polmear, *Acta Mater.* **45**, 3731 (1997).

[11] R. Ferragut, A. Somoza, A. Tolley, *Acta Mater.* **47**, 4355 (1999).

[12] A. Dupasquier, R. Ferragut, M.M. Iglesias, C.E. Macchi, M. Massazza, P. Mengucci, G. Riontino, A. Somoza, *Mater. Sci. Forum* **445-446**, 16 (2004).

[13] R. Ferragut, G. Ferro, M. Biasini, in: *Proc. 9th Int. Conf. on Aluminium Alloys*, Eds. J.F. Nie, A.J. Morton, B.C. Muddle, Institute of Materials Engineering Australasia Ltd, Melbourne 2004, p. 1022.